



# Aggregation-induced emission effect of hydrazinyldiphenyl sulfone central fluorophores



Wen Yang<sup>a</sup>, Jing Li<sup>a</sup>, Weiqun Zhou<sup>a,\*</sup>, Renyu Xue<sup>b</sup>, Zhongqing Cheng<sup>b</sup>, Mengying Li<sup>b</sup>, Haili Liu<sup>c</sup>, Youyong Li<sup>c</sup>

<sup>a</sup> School of Chemistry & Chemical Engineering and Material Science, Soochow University, 199 Ren'ai Road, Suzhou 215123, People's Republic of China

<sup>b</sup> School of Biology and Basic Medical Sciences, Soochow University, 199 Ren'ai Road, Suzhou 215123, People's Republic of China

<sup>c</sup> Functional Nano & Soft Materials Laboratory, Soochow University, 199 Ren'ai Road, Suzhou 215123, People's Republic of China

## ARTICLE INFO

### Keywords:

AIE effect

Hydrazinyldiphenyl sulfones

Aggregate states

V-shape molecule

Fluorescence staining

## ABSTRACT

We synthesized 4, 4'-Di ((E)-2-(4-4-aniline) hydrazinyldiphenyl sulfones (DHS1-4) of D- $\pi$ -A- $\pi$ -D and characterized them using NMR, IR, and element analysis. The investigation of photophysical properties in THF and aggregation-induced emission (AIE) effects in THF/H<sub>2</sub>O mixture solvent of these fluorophores were carried out respectively. DHS-4 displayed the strongest AIE effect in THF/H<sub>2</sub>O mixture solvent, and the value of  $I/I_0$  reached to 136. The nano-size aggregate states in THF/H<sub>2</sub>O mixture solvent of these compounds were determined by Scanning Electronic Microscopy (SEM) technology and fluorescent microscope imaging. AIE mechanism was explained by molecular dynamics (MD) simulation methods. The special packing manners of V-shape molecules can avoid effectively face-to-face  $\pi$ - $\pi$  stacking. The inter-molecular hydrogen bonding interactions affected the packing in the aggregate state and assisted their RIR (restricted intramolecular rotation) processes. Furthermore, living cell imaging of DHS-3 showed the bright blue fluorescence in A549 living cell. It indicates that DHS-3 can penetrate the cell membrane and aggregate in A549 living cell, which expands a new area to cell fluorescence staining.

## 1. Introduction

Organic photoimaging materials have attracted widespread interest in the past decade owing to a series of advantages in the fields of analytical, biological, medical sciences, etc. [1–3]. Among the diverse classes of organic conjugated systems [4–8], the materials absorb electromagnetic radiation by virtue of an intramolecular charge transfer (ICT) and emit from the corresponding photoexcited state. It is fascinating because of their notable applications in the field of molecular electronics, integrated photonic devices, non-linear optics (NLO), etc. [9–12]. The conventional structural design of organic fluorophores melds more and more aromatic rings together by increase the extent of  $\pi$ -conjugation to exhibit high fluorescence in the dilute solutions. The conventional organic dyes suffer from fluorescence quenching at high concentrations or aggregation state, which was known as the aggregation-caused quenching (ACQ) effects. The ACQ effect has restricted the real-world applications of fluorescent materials [13,14].

Since the first discovery of AIE phenomenon by Tang et al. [15], it has been extensively investigated for their potential application in

various fields. The AIE compounds provide a perfect way for overcoming the infamous ACQ effect of conventional organic dyes and make it possible for the practical applications of organic photoimaging materials [16–19]. The most convincing mechanism for the AIE is the restriction of intramolecular rotation (RIR) stacking molecules [20–23]. Of the hundreds functional AIE reported to date, most of them structurally composed by aromatic rigid building blocks preventing  $\pi$ - $\pi$  stacking, these groups could provide favorable 3D structures to RIR and benefit to AIE effects, such as *J*-aggregate formation, twisted intramolecular charge transfer, and conformational planarization [13,14,24].

Hexaphenylsilole (HPS) of a propeller shaped non-planar molecule [23] was the first unearthed silole derivatives of AIE phenomenon. BCPPM (3, 4-bis (4-(9-carbazolyl) phenyl)-N-methylmaleimide) with V-shaped D- $\pi$ -A- $\pi$ -D structure [25] was an excellent AIE material that exhibited large ICT fluorescent in the aggregation state. Hydrogen bonding is an important intermolecular interaction in supramolecular structures of the solid state. The formation of hydrogen bonds between luminogens can rigidify molecular structures and activate their RIR processes. This helps minimize the nonradiative energy losses of their

\* Corresponding author.

E-mail address: [wqzhou@suda.edu.cn](mailto:wqzhou@suda.edu.cn) (W. Zhou).

excitons and maximize their probability of radiative transitions [26]. D- $\pi$ -A- $\pi$ -D V-shaped BAHDS derivatives displayed AIE effect in mixture solvent [27] due to the intermolecular hydrogen bonds inhibited the intramolecular rotations and  $\pi$ - $\pi$  stacking. Inspired by BAHDSs, the designed strategies to enhance the AIE effect of the present contribution are to increase the intermolecular interaction such as hydrogen bonds and intramolecular charge transfer (ICT) effect at the molecular level and clarify further AIE mechanism. Here, four new D- $\pi$ -A- $\pi$ -D V-shaped compounds, 4, 4'-Di((E)-2-(4-4-aniline)hydrazinyldiphenyl sulfones (DHS1-4) were designed, which were based on the central acceptor sulfone unit, two hydrazinyldiphenyl  $\pi$ -bridge and four different donor units, amino, dimethylamino, methylphenylamino, and diphenylamino respectively. In light of the strong hydrogen bond ability of  $\text{NH}_2$  and larger substituent group effect such as diphenylamino, we investigate that the hydrogen bonding and large group effects impact on AIE effect. By means of AIE effect determination of fluorophores, we expect to obtain excellent AIE materials.

## 2. Experimental section

### 2.1. Materials and instruments

Bis(4-chlorophenyl)sulfone, hydrazine hydrate(85%), N-methyldiphenylamine, dimethyl formamide, phosphorus oxychloride, dichloromethane, triphenylamine, THF, DMSO, acetone, acetonitrile and  $\text{CDCl}_3$  were used as HPLC grade purchased from J&K (CHINA). Melting points were determined on a Kofler melting point apparatus and uncorrected. IR spectra were obtained in KBr discs using a Nicolet 170SX FT-IR spectrometer. Elemental analyses were performed on a Yancoo CHNSO Corder MT-3 analyzer.  $^1\text{H}$  NMR has been recorded on INOVA 400 at 400.13 MHz, with TMS as internal standard using DMSO- $d_6$  as deuterated solvents with chemical shifts reported as ppm. Mass spectra were recorded on a Finnigan MAT95 mass spectrometer. The absorption and fluorescence spectra were recorded on a CARY50 UV-vis spectrophotometer and an FLS920 fluorescence spectrophotometer. In this paper, the quantum yields of all compounds under air-saturated and nitrogen were investigated. Fluorescence quantum yields ( $\Phi_f$ ) in pure THF and THF/water mixtures were determined with anthracene ( $\Phi_f=0.27$ ) as the fluorescence reference in ethanol. The Quantum Yield (QY) of the as synthesized DHS derivatives was calculated based on the following equation [28], where standard (*std*) refers to the reference sample and unknown (*unk*) refers to compounds. *F* refers to the integrated fluorescence intensity, *A* refers to the absorbance; *n* is the refractive index of solvent, and  $\Phi$  is the quantum yield. Film samples for the measurements of UV-vis and fluorescence spectroscopy were prepared by drop casting and the subsequent spin-coating (2000 rpm, 30 s) from THF solutions (100 mL) on quartz cell (12.5  $\times$  12.5  $\times$  45 mm). The absolute fluorescence quantum yields in thin films were acquired on a Hamamatsu Quantaaurus-QY (C11347) instrument equipped with a CCD multichannel detector, an integrating sphere and xenon lamp excitation. Fluorescence decay times were determined with a time-correlated single-photon counting (SPC) fluorometer using a nanosecond flash lamp excitation source. For nanosecond lifetime measurements, the fluorescence decay curve was obtained by using an SPC apparatus (Edinburgh Analytical Instruments, FL-900CDT). A pulsed discharge lamp (pulse width  $\sim$ 1 ns, repetition rate 40 kHz) filled with hydrogen gas was used as the excitation light source. The emission light was detected by a photomultiplier tube (Hamamatsu, R955). The measured decay curves were analyzed on the basis of the deconvolution method. The results are presented in Fig. 1. The rate constant for radiative decay ( $k_r$ ) was calculated using equation (1):  $k_r = \frac{\Phi_f}{\tau}$ , While  $k_{nr}$ , i.e. the average non-radiative rate constant, was calculated using equation (2):  $k_{nr} = k_{tot} - k_r$ . Where  $k_{tot}$  is the total rate constant for decay ( $k_{tot} = 1/\tau$ ,  $\tau$  refers to the fluorescence lifetime). The fluorescence microscope imaging of the aggregations was obtained by

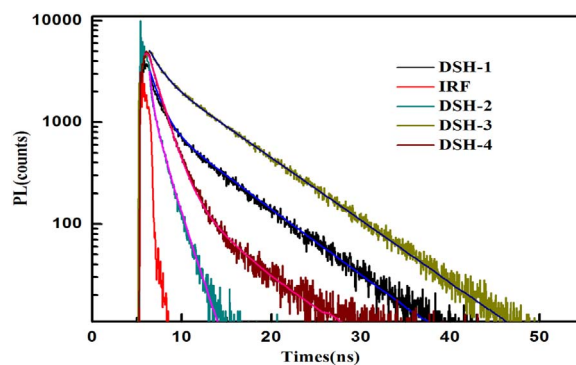


Fig. 1. The fluorescence lifetime of DHS-1 to DHS-4.

Leica DM2500M. The cell images were gathered with the inverted fluorescence microscope (Olympus, IX71) and processed with Nikon AY software. The scanning electron microscope (SEM) images of the aggregations were obtained by Hitachi S4800. All the experiments were carried out at room temperature.

### 2.2. Cell culture and fluorescence imaging

A549 cells (human lung adenocarcinoma cell) were purchased from the Shanghai Institute of Cell Biology. The cells were cultured in Roswell Park Memorial Institute culture medium (RPMI-1640), supplemented with 6% calf serum, penicillin ( $100 \text{ U mL}^{-1}$ ), streptomycin ( $100 \times 10^{-6} \text{ g mL}^{-1}$ ) and  $2.5 \times 10^{-4} \text{ mol L}^{-1}$  L-glutamine at  $37^\circ\text{C}$  in a 5%  $\text{CO}_2$  incubator. The cells were cultured in a 15 mm diameter cell culture dish for 2 days. A549 cells were incubated with the aggregations at a final concentration of  $50 \mu\text{g mL}^{-1}$  for 30 min, and washed with PBS buffer to remove extra cellular material. Then the dish was subjected to long-term imaging using an inverted fluorescence microscope (Olympus, IX71). The images were obtained at 450 nm ( $\lambda = 380 \text{ nm}$ ).

### 2.3. Computational methods

The ground and excited states of molecules were optimized with the Becke-3-Lee-Yang-Parr (B3LYP) [29–32] by density functional theory (DFT) and time-dependent DFT (TD-DFT) calculations at the level of 6-311G (d) with Gaussian 09 program [33]. SCRF (CPCM) method [34] at the same level was applied to indicate the dipole moments of the ground and the first excited state. Vibrational frequency calculations were also performed to ensure the stability of the calculation result and to avoid virtual frequency. The MD (molecular dynamic) simulations were performed by Discover module within Materials Studio 7.0 with the COMPASS force field for the studied molecules with the amorphous cell [35]. It was carried out with constant temperature and constant volume ensemble (NVT). Temperature was set 300 K and kept constant using a nose thermostat [36]. Pressure was set 1 atm. Electrostatic energies were calculated using the vdW & Coulomb method with a 9.5-Å non-bonded cutoff. The total simulation time of 10.0 ps was carried out with time step of 1.0 fs.

### 2.4. Synthesis

The general synthetic route for the synthesis of the compounds DHS-1, 2, 3 and 4 is depicted in Scheme 1. All compounds were synthesized in considerable yields. The precursors were readily obtained according to the literature procedures [37]. All new compounds were identified and characterized by elemental analysis, IR,  $^1\text{H}$  NMR, and  $^{13}\text{C}$  NMR spectroscopy.

#### 2.4.1. Synthesis of bis(4-hydrazinophenyl)sulfone

A mixture of bis(4-chlorophenyl)sulfone (5.74 g, 0.02 mol) and

Download English Version:

<https://daneshyari.com/en/article/5397792>

Download Persian Version:

<https://daneshyari.com/article/5397792>

[Daneshyari.com](https://daneshyari.com)